Wavelength demultiplexing optical switch

M. S. Ünlü, A. L. Demirel, S. Strite, S. Taşıran A. Salvador, and H. Morkoç
Coordinated Science and Materials Research Laboratories, Urbana, Illinois 61801

A novel wavelength demultiplexing optical switch (WDMOS) with completely optical input/output capabilities is demonstrated. The WDMOS input elements can be applied to optical logic circuits in which discrete wavelengths are utilized as an added dimension to the intensity levels of the optical signals. The WDMOS can be viewed as a resonant cavity-enhanced heterojunction phototransistor vertically integrated with a quantum well light emitting diode. The resulting device is an N-p-n-p optical switch situated in an optical cavity which serves to combine the wavelength selective spectral response of the optical cavity with the bistable switching characteristics of the N-p-n-p structure.

Increasing interest in digital optoelectronic circuits for optical communication systems and potential optical computing applications has created a demand for new device structures capable of optical input/output. Novel designs enabling multiple functions in a single device are desirable for reducing the complexity of optical receivers and transmitters as well as avoiding additional time delays due to interconnects. In this letter, we discuss an optoelectronic device combining two key photonic technologies: wavelength division multiplexing (WDM)[1] and optical switching.[2] The resulting device, the wavelength demultiplexing optical switch (WDMOS) consists of a resonant cavity-enhanced heterojunction phototransistor (RCEHPT),[3,4] vertically integrated with a quantum well (QW) light emitting diode (LED). We[5,6] and others[2,7–10] have previously described the optically induced switching in an N-p-n-p structure. The WDMOS extends these concepts by introducing the wavelength selectivity of the RCE-detection scheme. The resulting WDMOS devices are completely optical input/output switches which are sensitive not only to the intensity, but to the wavelength of the input signal.

Figures 1(a) and 1(b) show the schematic layer structure and the band diagram of the investigated device. The WDMOS was grown in a Perkin Elmer 430 molecular beam epitaxy machine on a p^+-GaAs (100) substrate. The structure can be viewed as an interwoven AlGaAs/GaAs N-p-n heterojunction bipolar transistor (HBT) and a GaAs p-n-p transistor [Fig. 1(a)]. The two $In_{0.2}Ga_{0.8}As$ quantum wells (QW) serve to confine carriers in the light emitting diode (LED). The entire structure is grown on a 10 period AlAs/GaAs quarter wave stack used as a high reflectivity mirror ($R_2 = 0.9$, center wavelength $\lambda \approx 950$ nm). The emission energy of the LED was chosen to be sufficiently small ($\lambda \approx 1$ μm) to avoid any feedback resulting from absorption in the N-p-n HBT. Another advantage of the InGaAs QW LED is that the optical output can be extracted through the quarter wave stack mirror as the GaAs substrate if such a configuration is desirable. Standard photolithography and wet etching techniques were used to fabricate three terminal devices for electrical characterization. Contacts to the n- and p-type layers were made by AuGe/Ni/Au and AuBe evaporations, respectively. A monochromatic light source was used for optical

measurements on devices fabricated with emitter windows.

The WDMOS is best viewed as an AlGaAs/InGaAs/GaAs RCEHPT driving an InGaAs/GaAs QW LED. The resonant cavity is formed between the buried AlAs/GaAs quarter wave stack mirror and the native GaAs surface [Fig. 1(a), $R_1 = 0.3$]. The HPT has a composite collector consisting of $In_{0.08}Ga_{0.92}As$ and GaAs regions. The InGaAs region serves to extend the photosen-
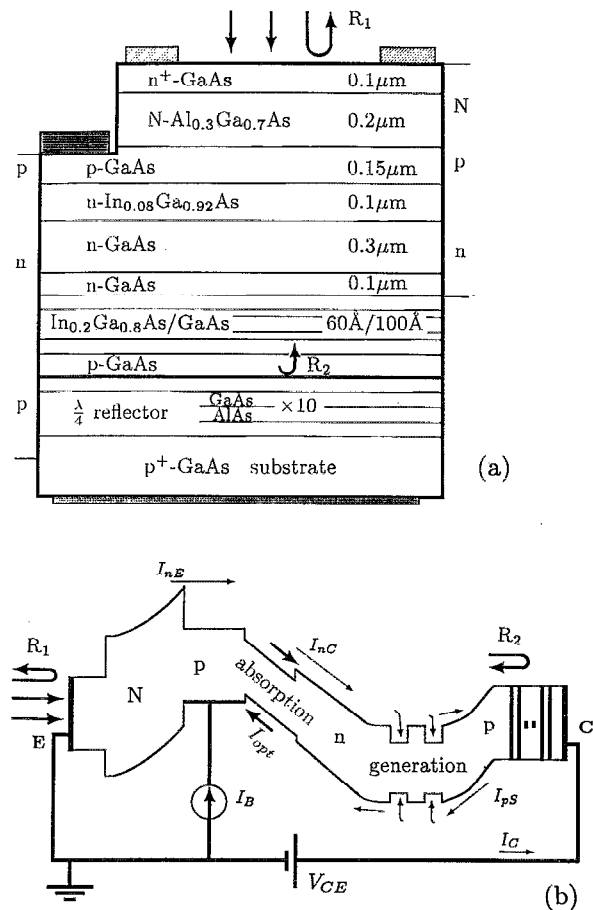

FIG. 1. (a) Schematic layer structure of the investigated devices. (b) Band diagram of the WDMOS in OFF state which displays various current components and optical interactions.
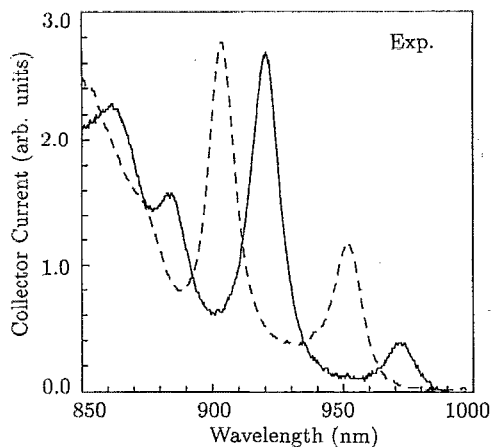
Downloaded 18 Jun 2002 to 128.197.180.119. Redistribution subject to AIP license or copyright, see http://ojps.aip.org/aplo/aplcr.jsp

FIG. 2. Spectral response of the WDMOS under monochromatic light for the as-grown structure (solid line) and after surface recessing (dashed line).

FIG. 3. Current-voltage characteristics of the WDMOS (emitter size $50 \times 50 \ \mu m$) as the base current is stepped. The inset shows the measured dependence of the collector current on the base current at constant collector-emitter bias ($V_{CE} = 5$ V).

sitivity spectrum to longer wavelengths (≈ 950 nm) in which absorption from the remainder of the structure is negligibly small. The field enhancement of the low loss optical cavity leads to large increases in the quantum efficiency of the HPT at the resonant wavelengths ($\approx 40\%$ for $0.1 \ \mu m$ InGaAs).[3] The wavelength spectrum of the HPT photosensitivity at low excitation power is shown in Fig. 2 for an as-grown device (solid line). The dashed line illustrates the shift in the resonant wavelengths of the cavity which is obtained when the top surface is recessed by wet chemical etching. For a given optical cavity length, the sensitivity is enhanced at resonance while the incident light is rejected by the cavity at off-resonance wavelengths,[3,4] which provides the wavelength selectivity of the WDM-OS. By changing the cavity length, the resonant wavelengths can be tuned within the range provided by the InGaAs absorption region and the AlAs/GaAs mirror. In this manner, arrays of WDMOS devices having complementary photosensitivities can be fabricated. For the devices shown in Fig. 2, the crosstalk of 1.0:4.3 at $\lambda = 904$ nm is limited by the low reflectivity of the GaAs top surface.[3]

In the structure described above, the vertical integration of the RCEHPT with the InGaAs/GaAs LED allows the HPT to drive the LED in an N-p-n-p configuration. The resulting device is a switch having a wavelength selective response to optical stimuli. The common-emitter current-voltage (I-V) characteristics of a $50 \times 50 \ \mu m$ emitter size WDMOS device are given in Fig. 3 for constant base current (I_B) steps. The inset shows the dependence of the collector current on the base current at constant collector-emitter voltage (V_{CE}). Note that, in the absence of base current, breakdown occurs at $V_{CE} > 16$ V. Dark current values of 6×10^{-6} and $< 10^{-4}$ A/cm^2 at $V_{CE} = 5$ V and $V_{CE} = 15$ V, respectively, were measured in devices fabricated without a base contact.

The three terminal device functions as an HBT in the low current regime (OFF-state). The measured collector current consists of holes injected from the p^+ substrate.
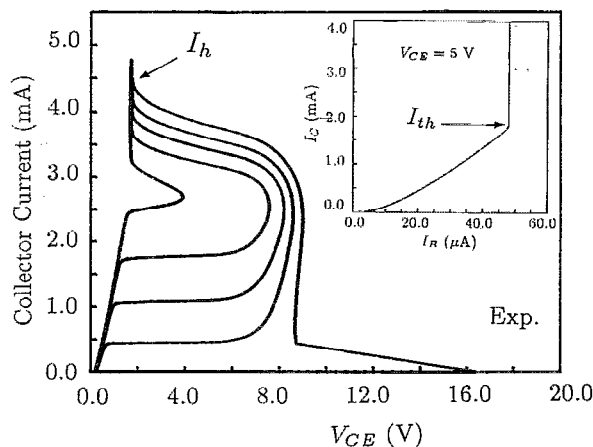
The electron current, injected from the emitter into the collector of the N-p-n transistor (I_{nC}) recombines with the holes (I_{pS}) from the p-n-p transistor in the InGaAs quantum wells generating light [Fig. 1(b)]. The holes which do not recombine in the quantum wells create additional base current constituting a positive feedback mechanism.

The current dependence of the N-p-n HBT gain can be seen in the Fig. 3 inset, which shows the superlinear increase of the collector current (I_C) with base current until the switching threshold is reached. The base current can be supplied either electrically through the base contact or optically from the carrier generation in the InGaAs collector region [I_{opt} Fig. 1(b)]. At the threshold, the collector current switches to a value limited only by the external circuit. The intensity of the optical excitation can be adjusted with regards to the switching threshold so that the switching is induced only by an excitation at the resonant wavelength. A large enhancement of the WDMOS collector current at the resonant wavelengths is then obtained as the device switches to the high current ON state. Depending on the external circuitry, the devices will remain ON or switch OFF after the excitation is removed. Self-resetting can be obtained if the ON state current level is smaller than the holding current I_h for zero bias (Fig. 3). When larger ON current levels are desired, the WDMOS can be switched OFF by removing the collector-emitter bias.

The evolution of the wavelength dependence of the collector current with the input excitation intensity can be computed from the measured photosensitivity (Fig. 2) and I_C-I_B dependence (Fig. 3 inset). It was necessary to calculate the WDMOS response at higher power excitations due to our lack of access to a tunable laser at the relevant wavelengths. The excitation was assumed to have a constant photon flux across the spectral range corresponding to approximately 90 μW [Fig. 4(a)] and 170 μW [Fig. 4(b)] at a 1 μm wavelength. The resonant peaks of Fig. 4(a) have larger peak to valley ratios compared with those in Fig. 2 as a result of the nonlinear dependence of the
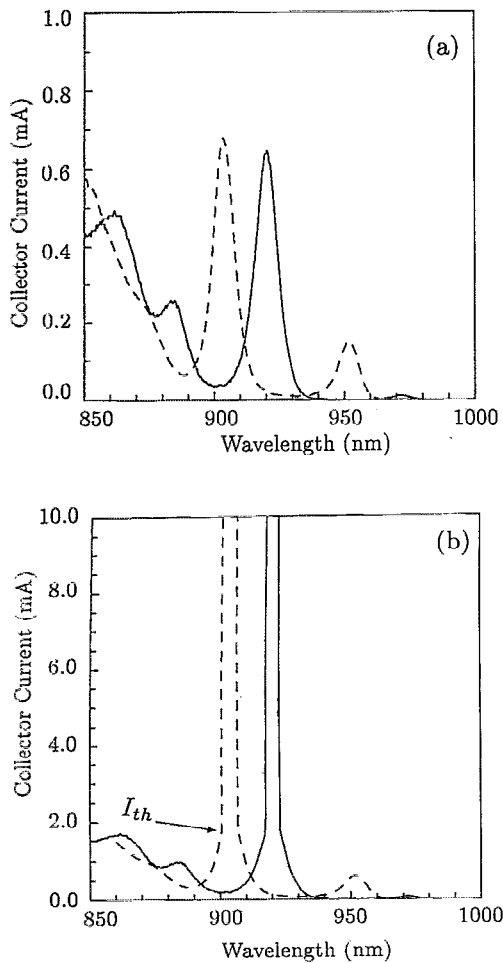
FIG. 4. Calculated spectral response of a $50 \times 50 \ \mu m$ emitter size WDM-OS device under constant input photon flux which is normalized to (a) 90 μW and (b) 170 μW at a wavelength of 1 μm. Note that the current level after switching is limited by the external circuit.

collector current on the base current (Fig. 3 inset). The basic device operation of the WDMOS can be seen in Fig. 4(b), in which the resonant optical intensity created a base current sufficient to surpass the WDMOS switching threshold, resulting in a drastic increase in the amount of the collector current. When an array of WDMOS devices are illuminated at a particular wavelength, only those devices tuned into resonance with the excitation will switch.

We can imagine a number of optoelectronic logic and memory elements which can be constructed from WDM-OS devices in which not only the intensity of the optical signal, but its wavelength, is also a parameter. For example, two adjacent WDMOS devices electrically connected in series would function as an AND for the two resonant wavelengths. If they are connected in parallel, the resulting function would then be an OR gate. The wavelength selectivity of the WDMOS design will allow higher packing densities to be achieved by relaxing the limitations imposed by crosstalk between neighboring devices. In the present

structure, the broadband output light signal does not allow cascadability of WDMOS devices. For the direct application of the WDMOS to purely optical logic circuitry, the WDMOS needs to drive narrow band light sources (e.g., surface emitting lasers) which emit at wavelengths included in the set of input excitations.

In a WDM device, the number of available channels is limited by the finesse of the resonant cavity. The cavity formed by using the GaAs surface as the top mirror offers a full width at half-maximum (FWHM) of 15 nm and the finesse is limited to less than 4 for practical cavity lengths.[4] A significant improvement in the wavelength selectivity can be obtained by increasing the top mirror reflectivity.[3] A FWHM of 3 nm was demonstrated for a HPT integrated in a resonant cavity formed with two periodic reflectors.[11] For such a high finesse structure, it should be possible to obtain more than 10 channels within the accessible spectrum of the strained InGaAs/GaAs system.

In conclusion, we have demonstrated a novel wavelength selective optoelectronic switching device with completely optical input/output capabilities. The wavelength demultiplexing optical switch (WDMOS) device can be viewed as a resonant cavity-enhanced heterojunction phototransistor (RCEHPT) which drives an InGaAs/GaAs light emitting diode (LED), or equivalently, as an N-p-n-p optical switch situated in an optical cavity. The superlinear dependence of the collector current on the base current enhances the wavelength dependent output of the RCE-HPT. In turn, the optical cavity adds a new dimension, wavelength selectivity, to the input parameters of the N-p-n-p optical switch. If multiple wavelength output elements can be developed, it should be possible to use the WDM-OS input elements in optical logic circuitry in which the wavelength, in addition to the intensity of the optical excitation, can be used as an input parameter.

[1] H. Ishio, J. Minowa, and K. Nosu, IEEE J. Lightwave Technol. 2, 448 (1984).
[2] K. Matsuda and J. Shibata, IEEE Proc. 138, 67 (1991).
[3] K. Kishino, M. S. Ünlü, J.-I. Chyi, J. Reed, L. Arsenault, and H. Morkoç, IEEE J. Quantum Electron. 27, 2025 (1991).
[4] M. S. Ünlü, K. Kishino, J.-I. Chyi, J. Reed, L. Arsenault, and H. Morkoç, Electron. Lett. 26, 1857 (1990).
[5] M. S. Ünlü, S. Strite, A. Salvador, and H. Morkoç, Inst. Phys. Conf. Ser. (in press).
[6] M. S. Ünlü, S. Strite, A. Salvador, A. L. Demirel, and H. Morkoç, IEEE Photon. Technol. Lett. 3, 1126 (1991).
[7] G. W. Taylor, R. S. Mand, J. G. Simmons, and A. Y. Cho, Appl. Phys. Lett. 49, 1406 (1986).
[8] F. R. Beyette Jr., S. A. Feld, X. An, K. M. Geib, M. J. Hafich, G. Y. Robinson, and C. W. Wilmsen, Electron. Lett. 27, 497 (1991).
[9] H. Beneking, N. Grote, W. Roth, and M. N. Svilans, Electron Lett. 59, 1600 (1991).
[10] James F. Gibbons, IEEE Trans. Electron. Devices 11, 406 (1964).
[11] R. P. Bryan, G. R. Olbright, W. S. Fu, T. M. Brennan, and J. Y. Tsao, Appl. Phys. Lett. 59, 1600 (1991).